

## USE OF CATION-EXCHANGE TO PRODUCE HIGHLY DISPERSED IRON CATALYSTS IN LOW RANK COALS

M. Mehdi Taghiei, F. E. Huggins, B. Ganguly, and G. P. Huffman  
IMMR/CFFLS, University of Kentucky, Lexington, KY, 40506.

### Abstract

A significant enhancement of both liquefaction yields and desirable products from two lignites has been achieved by incorporating iron in the lignites by an ion-exchange process. At 5-8% iron content, total conversions approached 88% and oil yields were about 45% compared to 62% total conversion and 33% oil yield for the raw coal. The effect of catalyst loading on cation-exchanged lignites was studied to determine the concentration that results in the optimum oil yield.  $^{57}\text{Fe}$  Mössbauer and XAFS spectroscopies were used to characterize the catalyst structure and size distribution in the iron cation-exchanged lignites before and after liquefaction. The results indicate that the added iron is initially present in bimodal form, with most present as highly dispersed goethite ( $\alpha\text{-FeOOH}$ ) particles, 50-100Å in diameter, but with a significant fraction (about 30%) of the iron in particles less than 30Å in diameter, which may represent molecularly dispersed ferric ions at the ion-exchange (carboxyl) sites. With sufficient sulfur present in the system, the iron is rapidly transformed to pyrrhotite ( $\text{Fe}_{1-x}\text{S}$ ) during liquefaction.

### Introduction

A number of studies<sup>1-3</sup> have been conducted on the activity of various iron-based catalysts during liquefaction of coals of different rank. Recent research<sup>4</sup> has shown that sulfated iron catalysts can significantly enhance the conversion yield of high-rank coals. However, for lower rank coals, the improvement in conversion yield through the addition of similar sulfated catalysts has not yet been achieved. The oxygen contents of low-rank coals such as lignites are significantly higher than those of high-rank coals, and as a result, oil yields from liquefaction of low-rank coals tend to be low due to  $\text{CO}_2$  formation. A considerable portion of this oxygen derives from carboxyl groups and other oxygen functional groups. In low-rank coals, most of the exchangeable cations are associated with carboxyl groups, and a number of studies<sup>5,6</sup> have shown that the behavior of lignites in coal conversion processes is greatly affected by the amount and type of exchangeable cations present.

The results of this study indicate that iron ion-exchanged into the low-rank coals constitutes a catalyst in a state of dispersion ranging from molecular ions to particles a few nanometers in diameter. Superparamagnetic modeling of Mössbauer spectra<sup>7</sup> indicates that the iron particle size in a high-iron loaded lignite has a bimodal character, with the majority of the particle sizes ranging from 50 to 115Å in goethite form, but with a significant fraction (about 30%) less than 30Å, which may derive from ferric cations in ion-exchange sites bound to the oxygen anions of carboxyl groups. The direct coal liquefaction (DCL) total conversion and oil yields of the iron ion-exchanged Beulah and Hugel lignites used in this work were enhanced significantly compared to the raw lignites.

## Experimental

The two lignites used in this study are Beulah (obtained from Dept. of Energy Coal Sample, DECS-11) and Hagel (obtained from Pen. State Office of Coal, PSOC-1482) from the Fort Union region in North Dakota. The original iron contents of these lignites are less than 0.5 percent. The ion-exchange experiments were carried out in a 10 liter fermenter using a freshly made 0.05M aqueous solution of ferric acetate at a controlled pH of about 2.8 and a constant temperature of 60°C. The iron contents of the Beulah and Hagel lignites after the ion-exchange process were 7.8% and 5.33%, respectively. The efficiency of lower loadings (~1 wt%) of iron in the ion-exchanged lignites during liquefaction was also investigated.

### Liquefaction Experiments:

Two sets of coal liquefaction experiments were conducted. The first set of experiments was carried out with tubing bombs in a fluidized sand bath. This set of experiments was designed to investigate the effect of iron catalysts on the total yield and product distribution in the liquefaction process. The tubing reactor was first charged with a slurry mixture of lignite and tetralin in a 1:2 ratio in the presence of dimethyl disulfide (DMDS) as a sulfur donor, and pressurized to 800 psi (cold) with hydrogen. Control liquefaction experiments, using slurry mixtures of the same lignite samples with a 30Å iron oxide and with no catalyst, were run under the same conditions to compare the catalytic effects of an ultrafine particle iron oxide with those obtained for the ion-exchange catalyst. The products were separated into THF insoluble organic materials (IOM), THF soluble, toluene insoluble (preasphaltene), toluene soluble, pentane insoluble (asphaltene), and pentane soluble (oil and gas) fractions. The soluble product percentage yields were calculated on a dry, ash-free (daf) basis as follows:

$$\text{Percentage soluble products} = \frac{\text{total soluble products}}{\text{daf lignite}} \times 100$$

Pentane solubles were determined by subtracting the sum of asphaltenes, preasphaltenes and the IOM residue from the weight of the starting lignite. The results were reproducible within ±2%.

The second set of experiments was designed to generate larger samples for the detailed characterization of the chemical structure and reactions of the added iron. The apparatus used to prepare the samples for these experiments was an one liter autoclave. This autoclave was connected at the top to a vessel for holding the sample prior to heating. At the bottom, four nitrogen-purged sampling lines were attached to the outlet valve of the autoclave to collect the liquefaction products directly from the autoclave without exposure to air. Liquefaction experiments in the autoclave were performed at 385°C and 400°C under 1500 psi of hydrogen pressure (cold) in the presence of excess tetralin (tetralin:coal 3:1) and dimethyl disulfide (DMDS) as a sulfur donating species.

### Mössbauer and XAFS Spectroscopies:

Mössbauer spectra for the as-received, demineralized, and ion-exchanged lignite samples were obtained using a conventional constant-acceleration-type Mössbauer spectrometer<sup>8</sup>. The samples were run at several temperatures to determine the size distribution. Calculation of the particle size distribution is described in detail elsewhere<sup>7</sup>. XAFS measurements were performed at beam line X-19A at the National Synchrotron Light Source in Brookhaven National Laboratory. Iron K-edge XAFS spectra of the samples were obtained in transmission mode using a Si(111) double crystal monochromator.

### Results and Discussion

The effect of iron concentration on liquefaction yields of Beulah and Hagel coal is shown in Figure 1. It can be seen that the asphaltene and oil conversion yields increased significantly for both ion-exchanged lignites compared to the raw coals. The preasphaltene yields, however, tend to decrease as a result of catalyst addition to the lignite. We have also compared the results obtained using a physically added 30Å iron oxyhydroxide catalyst to those obtained using cation-exchanged iron at approximately the same concentrations. The 30Å iron oxyhydroxide catalyst was provided by Mach I Inc., and its interesting structural properties are discussed in several forthcoming publications<sup>9,10</sup>. It is evident from Figure 1 that the ion-exchanged iron is a more active catalyst than the 30Å iron oxide.

Mössbauer and XAFS spectroscopies were used to characterize the structure of the cation-exchanged iron both before and after DCL. The characterization of iron-based DCL catalysts by Mössbauer and XAFS spectroscopies has been discussed in detail elsewhere<sup>11</sup>. The Mössbauer spectra of the Beulah and Hagel lignites containing cation-exchanged iron are shown in Figures 2 and 3, respectively. The spectra are fit with one or several magnetic components and quadrupole doublets (peak positions denoted by bar diagrams), and a superparamagnetic relaxation component (dashed curve). As discussed by Ganguly et al.<sup>7</sup>, at a given temperature, particles with diameter less than some critical value will give rise to a quadrupole doublet, particles with a diameter greater than some larger critical value will exhibit a six-peak magnetic hyperfine spectrum, and particles with diameters between these two values will give rise to superparamagnetic spectra. Approximate size distributions can be determined by measuring the percentages of these three components as a function of temperature and the size distribution determined in this manner for the cation-exchanged Hagel lignite with 5.33% Fe is shown in Figure 4. It is seen that the size distribution is bimodal, with approximately 70% of the particles in the 50-100Å size range, and 30% having diameters less than 30Å. Much of the iron in the latter size category may in fact be ferric iron that is molecularly dispersed and bonded to oxygen anions of the carboxyl groups in the lignite, whereas, the larger particles result from hydrolysis of either iron acetate or ion-exchanged iron to form goethite. The low-iron cation-exchanged coals exhibit similar Mössbauer spectra, but a detailed study of the temperature dependence of the superparamagnetic relaxation spectra has not yet been completed. Nevertheless, it is evident that most of the iron in these samples is contained in iron oxyhydroxide particles less than 100Å in diameter, and a significant percentage of the iron is present in the less than 30Å diameter size category.

Both the x-ray absorption near edge structure (XANES) and the radial structure function (RSF) derived from the iron K-edge XAFS spectra of the iron loaded lignites exhibit significant size related effects. Typical results are shown in Figure 5. The XANES of the Hagel lignite sample is compared to that of bulk goethite in Figure 5a, while the corresponding RSF are compared in Figure 5b. It is seen that the XANES of the iron loaded Hagel lignite sample and goethite are quite similar, with the exception of an increase in the intensity of the small pre-edge peak. This occurs because the surface iron atoms of ultrafine ferric oxide particles are no longer in centrosymmetric octahedral coordination, but in reduced coordination number sites, which cause the intensity of the pre-edge ( $1s \rightarrow 3d$ ) transition to increase. The RSF of the Hagel lignite sample and goethite exhibit similar peaks, but the peaks corresponding to the iron shell are decreased in amplitude for the iron in the lignite, consistent with a small particle size<sup>11</sup>.

Further studies are in progress (i) to determine the structure and size distribution of the cation-exchanged iron as a function of concentration, both before and after liquefaction, (ii) to investigate the use of the cation-exchange process for preparation of small particle metal oxides containing Mo, Co, Al, Ni, etc., and (iii) to evaluate the potential of these ion-exchange catalysts for lignite liquefaction.

#### Acknowledgement

This research was supported by the U.S. Department of Energy through DoE contract No. DE-FC22-90-PC90029 as part of the research program of the Consortium for Fossil Fuel Liquefaction Science.

#### References:

- 1- Herrick, D. E.; Tierney, J. W.; Wender, I.; Huffman, G. P.; Huggins, F. E. *Energy & Fuels* **1991**, *4*, 231.
- 2- Tanabe, K.; Yamaguchi, T.; Hattori, H.; Sanada, Y.; Yokoyama, S. *Fuel Proc. Technol.* **1984**, *8*, 117.
- 3- Cook, P.S.; Cashion, J. D. *Fuel* **1987**, *66*, 661.
- 4- Pradhan, V. R.; Tierney, J. W.; Wender, I.; Huffman, G. P. *Energy & Fuels* **1991**, *5*, 497.
- 5- Matsumoto, S.; Walker Jr., P. L. *Carbon* **1986**, *25*, 277.
- 6- Linares-Solano, A.; Hippo, E. J.; Walker Jr., P. L. *Fuel* **1986**, *65*, 776.
- 7- Ganguly, B.; Huggins, F. E.; Rao, K. R. P. M.; Huffman, G. P. *J. Catalysis*, **submitted**.
- 8- Huffman, G. P. *Chemtech.* **1980**, *10*, 504.
- 9- Ganguly, B.; Huggins, F. E.; Feng, Z.; Huffman, G. P. *Phys. Rev.*, **submitted**.
- 10- Zhao, J.; Huggins, F. E.; Feng, Z.; Lu, F.; Shah, N.; Huffman, G. P., *J. Catalysis*, **submitted**.
- 11- Huffman, G. P.; Ganguly, B.; Zhao, J.; Rao, K. R. P. M.; Shah, N.; Feng, Z.; Huggins, F. E.; Taghiei, M. M.; Lu, F.; Wender, I.; Pradhan, V. R.; Tierney, J. W.; Seehra, M. S.; Ibrahim, M. M.; Shabtai, J. S.; Eyring, E. M., *Energy & Fuels* **1992**, in press.

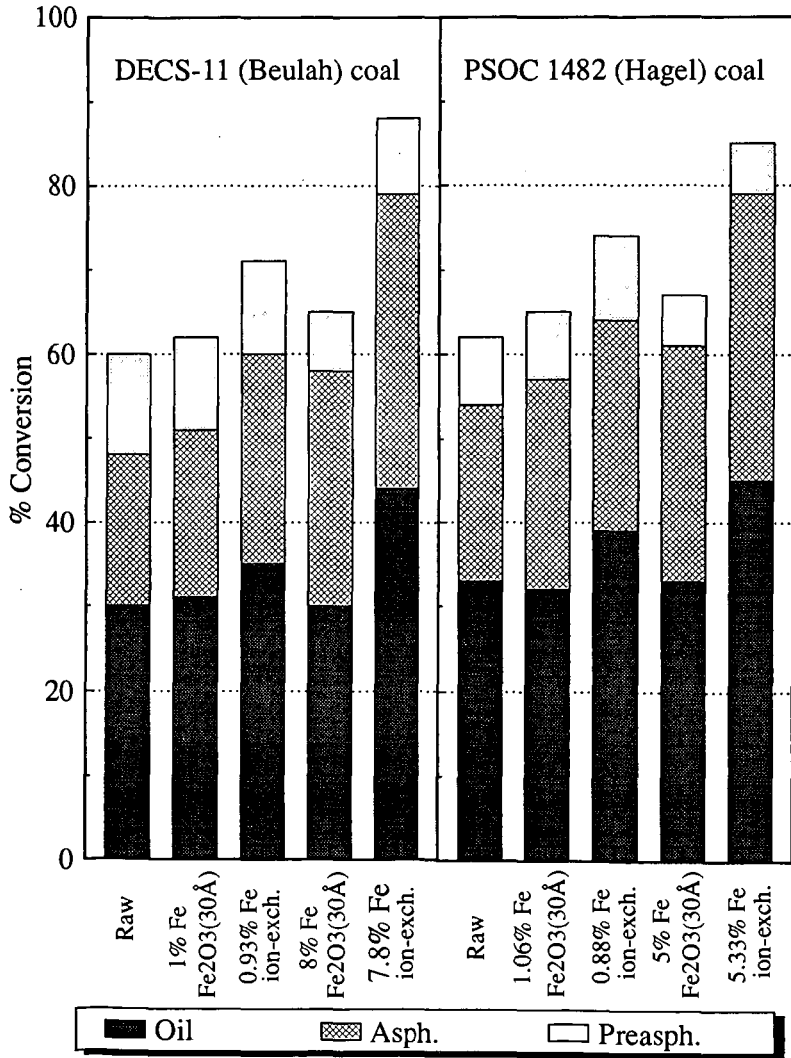


Figure 1. Comparison of liquefaction product yield for Beulah and Hagel lignites

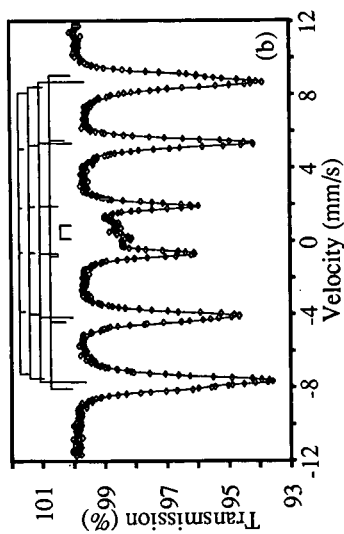
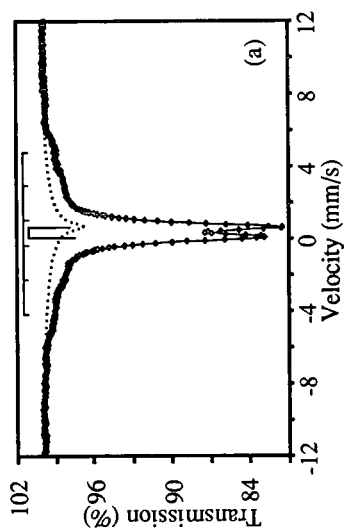


Figure 2. Mössbauer spectra of ion-exchanged Beulah lignite with 7.8% iron, (a) at room temperature, (b) at 12K.

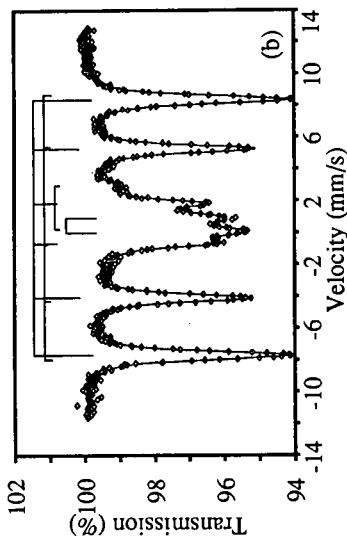
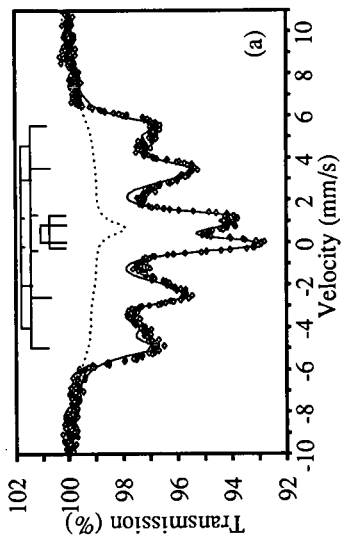


Figure 3. Mössbauer spectra of ion-exchanged Hagel lignite with 5.33% iron, (a) at room temperature, (b) at 12K.

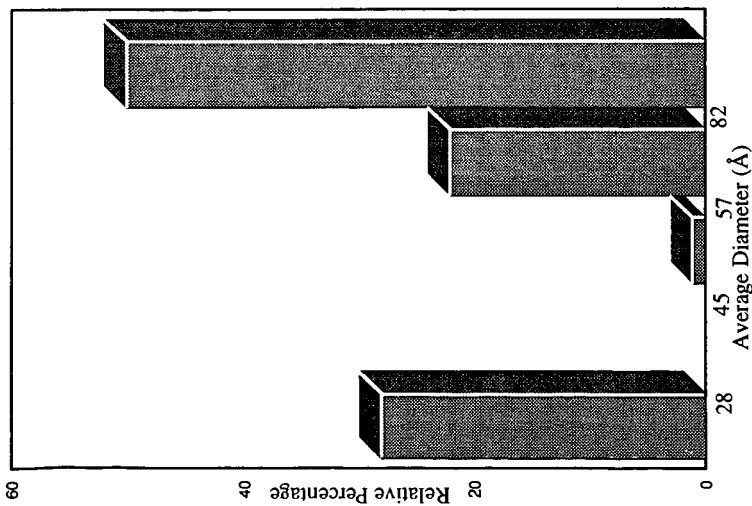


Figure 4. Size distribution of iron species in Hagel lignite containing 5.33 wt% iron.

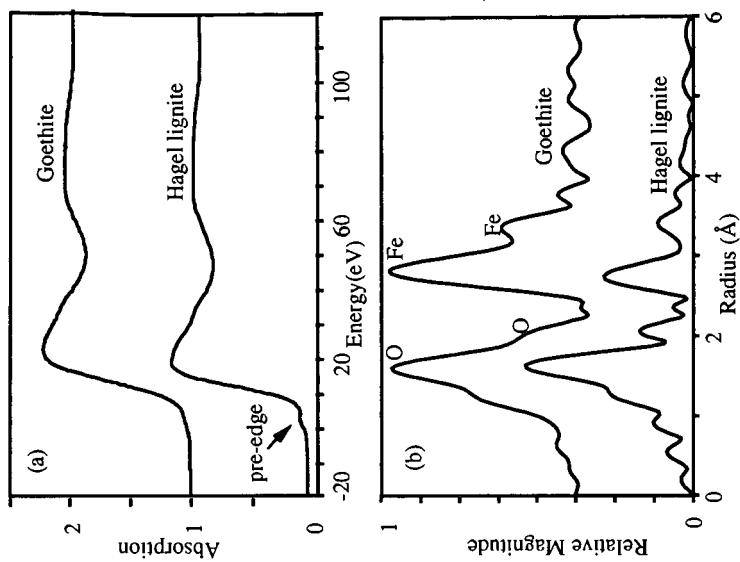


Figure 5. Comparison of iron K-edge (a) XANES, and (b) RSF of bulk goethite and iron loaded Hagel lignite.

## OPTIONS FOR IRON-CATALYZED LIQUEFACTION OF LOW-RANK COALS

Edwin S. Olson, Candace M. Buchwitz, and Mary Yagelowich  
Universal Fuel Development Associates, Inc.  
Grand Forks, ND 58201

Ramesh K. Sharma  
University of North Dakota Energy and Environmental Research Center  
Grand Forks, North Dakota 58202

Key Words: Coal liquefaction, iron catalysts, ion exchange

### ABSTRACT

Liquefaction of low-rank coals is impeded by the mineral content of the coal. Inorganic constituents such as calcium are a major factor in deposits in the process equipment, but they also disrupt the functioning of the catalyst by blocking pores, deactivating sites, or causing sintering or aggregation. A series of liquefaction tests was performed that compared ion-exchanged Wyodak coal with the as-received coal. The catalysts were impregnated iron or iron dispersed on acidic supports. Highest conversions to heptane solubles were obtained with iron impregnated (PETC method) into acid-washed Wyodak. Alternatively, solubilization of as-received Wyodak with CO/water (uncatalyzed) gave an ash-free intermediate that produced high conversions to heptane-soluble product in the subsequent catalyzed liquefaction reaction.

### INTRODUCTION

The high calcium content of low-rank coals has been recognized for some time as a potential problem in processing these coals to useful products. Operational difficulties were experienced at the Wilsonville Advanced Coal Liquefaction Research and Development Facility during the runs with Black Thunder (Wyoming) subbituminous coal due to substantial solids deposition (1). These deposits contained large amounts of calcium carbonate. In batch and continuous unit tests conducted at PETC (2), dispersed iron catalysts prepared by the PETC method exhibited poorer activities with subbituminous coals than previously obtained with bituminous coals. Swanson (3) recently reported that deposits of calcium coated the dispersed catalyst particles during tests with Black Thunder coal. Joseph and Forrai (4) examined the adverse effects of exchangeable cations (Na, K, Ca) on liquefaction of low-rank coals by ion-exchanging additional ions into the coals. The evidence cited in these reports implies that calcium deposits can rapidly deactivate the catalyst by blocking pores and active sites in the fine particles or could cause the particles to aggregate. Loss of catalytic activity for the activation of hydrogen then leads to condensation and retrograde reactions that form carbonaceous deposits and low oil yields.

Replacement of the alkaline earth cations with hydrogen ions is a possible solution. However, previous studies at EERC (5) demonstrated that noncatalytic thermal liquefaction of acid-washed lignite gave lower

conversions than the as-received coals. The lower yields were attributed to condensation reactions catalyzed by the highly acidic clays generated during the exchange process. Recently the conversions of coals washed with methanolic HCl were examined (6). This pretreatment significantly increased the conversion to THF-solubles in noncatalytic reactions. The significant increase in conversion to oils for ammonium-exchanged lignite (4) also demonstrates the potential for metal cation removal but may not be feasible for catalytic processing because of release of the ammonia. The behavior of acid-exchanged and other demineralized low-rank coal materials in liquefaction with various types of dispersed catalysts requires extensive investigation and elucidation.

This paper reports our investigations on the catalytic liquefaction of low-rank coal that was pretreated by ion exchange with aqueous acid and by thermal solubilization to a mineral-free product. A series of tests with ion-exchanged Wyodak subbituminous coal (IEW) was conducted to determine the effectiveness of various dispersed iron catalysts without the complications of the exchangeable cationic components. A second objective was to examine an alternative liquefaction scheme that produces mineral-free low-severity intermediate in a noncatalytic thermal pretreatment stage, that is subsequently liquefied with various dispersed iron catalysts in hydrogen.

## EXPERIMENTAL

### Preparation of Ion-Exchanged Coals

Acid-washed Wyodak (IEW) coal was prepared by stirring 7 g of ARW in 100 ml 1N nitric acid for one hour at ambient temperature. The acid-treated coal was separated by centrifugation and washing with water.

### Coal Liquefaction

As-received Wyodak-Clovis Point (ARW) and IEW coals were pretreated using several different techniques prior to liquefaction. The PETC-method (7) was used for both ARW and IEW. Procedures reported by Ziolo and coworkers (9) were modified to prepare  $Fe_2O_3$  dispersed on the coals. A slurry consisting of 7.0 g of ARW coal or product coal obtained from pretreatment of 7.0 g ARW, 10 wt% of catalyst (if required), 0.1 g of elemental sulfur, and 14 g of tetralin (solvent) were placed in a 70-ml Parr reactor. The reactor was evacuated and charged with 1000 psi (initial) of hydrogen gas. The reactor was heated to 425°C in a rocking autoclave (initial heatup time = 15 minutes) and left at this temperature for 60 minutes. At the end of the reaction, the reactor was cooled to room temperature, and the gases were removed. The product slurry was extracted with tetrahydrofuran (THF). The THF-insoluble product was dried under vacuum and weighed. A 4 ml aliquot of the THF-soluble was mixed with one ml solution of internal standard (a mixture of 2,2,4-trimethylpentane and n-octadecane in dichloromethane) and analyzed by GC. The remaining THF-solubles were evaporated to remove THF, and the dark oil was added to a large excess of heptane and stirred. The heptane-insoluble product was separated by centrifugation, washed with heptane, dried in vacuo at 50°C and weighed. The percent conversion was calculated on the basis of the coal (maf) that did not appear in the THF-insoluble fraction. Heptane-soluble yields were obtained by difference (100% - %THF-insolubles - %heptane-insolubles).

## RESULTS AND DISCUSSION

Wyodak subbituminous coal was treated with nitric acid to remove by ion-exchange the metal cations bound to the coal matrix. Initial thermal (noncatalytic) tests were carried out to provide a basis for comparison with the catalytic tests. These tests required heating the coal/tetralin slurry in a rocking microtube reactor for 1 hr at 425 °C with 1000 psi (cold pressure) of hydrogen. Conversion and yield data are given in table 1. The thermal reaction of as-received Wyodak coal (ARW) gave a very high conversion (89%) to THF-soluble products. These data are consistent with earlier results for low-rank coals in thermal (noncatalytic) reactions in hydrogen or carbon monoxide (5). Carbon monoxide works as well as hydrogen in the noncatalytic reactions. The conversion for the (IEW) test (86%) was lower than that for the ARW coal on a maf basis. The lower conversion is also consistent with earlier work with low-rank coals that demonstrated that acid-washing lowers the conversion. This effect was attributed to the generation of highly acidic sites on clay minerals in the coal that catalyze carbonium ion reactions that often result in condensations to higher molecular weight and less soluble products. The amounts of heptane-soluble products formed in the two thermal reactions were similar (48%). The heptane-soluble yields are obtained by difference (100% - %THF-I - %heptane-I) and include major amounts of the gaseous products (CO<sub>2</sub>, H<sub>2</sub>O, etc.) in addition to the heptane-soluble oils.

The ion-exchanged coal was then reacted in catalytic liquefaction tests with several dispersed iron catalysts, and these results were compared with similar catalytic reactions carried out with the ARW in order to determine the effect of the inorganic cations on the catalytic activity. The PETC method (7) for impregnating iron as the iron hydroxyoxide on the coal surface was utilized for preparing the dispersed iron catalyst for liquefaction of both ARW and IEW coals. Addition of iron hydroxyoxide to ARW via the PETC method resulted in a conversion to THF solubles similar to those found in the thermal reactions (88%), but the yield of heptane-solubles was substantially higher (52%). Thus the catalytic effect is demonstrated principally in the oil yield. Generation of iron hydroxyoxide on the IEW significantly improved the conversion THF-solubles as well as heptane-solubles (56%). The significant increase in yields for the IEW can be attributed to less deactivation of the catalyst by the inorganic matter.

Alternative methods for generating dispersed iron on the coal surface were also examined. Previous work at Universal Fuel Development Associates, Inc. (8) demonstrated that clay-supported iron catalysts with high concentrations of maghemite fine particles were much more catalytically active than those with hematite. Ziolo and coworkers (9) reported that maghemite fine particles can be generated on ion-exchange resins by reducing ferric ions with hydrazine and sodium hydroxide or by treating ferrous ions with hydrogen peroxide and ammonium hydroxide. Since sodium hydroxide dissolves humic acids from the low-rank coal, ammonium hydroxide was utilized instead of sodium hydroxide to prepare the maghemite fine particles on the coal surface. Treatment of the coal with ferrous chloride/ammonium hydroxide to maximize maghemite formation did not improve conversions for IEW, 92% to THF-solubles, 47% heptane-solubles. Likewise treatment with ferric nitrate/hydrazine did not improve conversions, 91% THF-solubles, 46% heptane-solubles. A reaction carried out with this same pretreated coal but

Table 1  
Catalytic Liquefaction with Dispersed Iron

Reaction Temp. = 425°C, Reaction Time = 1 hr, H <sub>2</sub> = 1000 Psi (cold) Wyodak (AR) coal = 7.0 g., Coal/Tetralin = 0.5, Sulfur = 0.15 g.				
Pretreatment	Conv. (%)	THF-I (%)	Heptane-I (%)	Heptane-S (%)
None*	89	11	41	48
Acid washed*	86	13	40	47
Fe(NO <sub>3</sub> ) <sub>3</sub> + NH <sub>4</sub> OH <sup>a</sup>	88	12	36	52
1 Acid washed 2 Fe(NO <sub>3</sub> ) <sub>3</sub> + NH <sub>4</sub> OH <sup>a</sup>	91	9	36	56
1 Acid washed* 2 Fe(NO <sub>3</sub> ) <sub>3</sub> + N <sub>2</sub> H <sub>4</sub> + NH <sub>4</sub> OH <sup>b</sup>	88	12	43	45
1 Acid washed 2 Fe(NO <sub>3</sub> ) <sub>3</sub> + N <sub>2</sub> H <sub>4</sub> + NH <sub>4</sub> OH <sup>b</sup>	91	9	45	46
1 Acid washed 2 FeCl <sub>2</sub> + NH <sub>4</sub> OH + H <sub>2</sub> O <sub>2</sub> <sup>b</sup>	92	8	45	47

\* = No sulfur was added to the reaction mixture.

a = PETC method.

b = Modified Ziolo method.

without addition of sulfur gave a similar conversion, indicating that the iron dispersed by this method is inherently inactive.

Previous work in this project was concerned with the preparation of fine iron sulfide particles supported on an acidic clay, and a preliminary report of mixed iron/alumina-pillared montmorillonite catalysis was presented (8). Catalytic liquefaction reactions of ARW and IEW were performed in tetralin using conditions similar to those above. Reactions were carried out using 10 wt% of the clay catalysts (sulfided in situ using small amount of elemental sulfur) at 425°C for one hour in 1000 psi of initial hydrogen pressure. The reaction conditions and yields data are given in table 1.

With the most active of the mixed iron/alumina-pillared clay catalysts in the presence of sulfur, the conversion of the ARW was 91% to THF-solubles with 53% heptane solubles. In the absence of sulfur required for sulfidation of the oxyiron catalyst, the conversion was substantially less, 87% to THF-solubles, with only 33% heptane-solubles. This large reduction in oil yield is attributed to the presence of the highly acidic clay and absence of any good hydrogen activation capability. The reaction of IEW coal with the active sulfided clay catalyst gave a significantly higher conversion to THF solubles, and excellent conversion to heptane-solubles (54%).

Although significant improvements in oil yields were obtained as a result of pretreating the Wyodak to remove metal cations, the economics of an ion-exchange process and subsequent disposal of the acidic waste water may not compensate for the increase in conversion and operability. An alternative liquefaction process has been utilized for many years at the Energy and Environmental Research Laboratories. This processing involves a noncatalytic thermal pretreatment under carbon monoxide atmosphere to break down the cross-links in the coal to give a high molecular weight THF-soluble intermediate in 95% yield. Mineral matter is conveniently removed from the coal solution. This cation-free low-severity intermediate is then used in catalytic liquefaction tests with hydrogen.

Several reactions of a mineral-free low-severity intermediate from Wyodak coal (LSW) were carried out with dispersed iron catalysts. A THF-soluble intermediate was obtained by thermal liquefaction in CO and was separated from heptane-soluble products and solvent(tetralin)-derived materials by solvent (heptane) precipitation to give the high molecular weight LSW intermediate for these tests. The LSW is a low-density solid at ambient temperature, but melts easily. A thermal (noncatalytic) reaction of the LSW in tetralin at 425 °C for 1 hr in 1000 psi hydrogen gave 15% conversion to heptane-solubles (Table 3). The conversions obtained for the LSW substrate cannot be directly compared with the coal conversions above, because the substrates are quite different. The 15% value for the LSW substrate represents a conversion of preasphaltenes and asphaltenes to heptane-soluble oils, whereas the 48 to 54% yields of heptane-solubles given above for coal substrates include both the more easily cleaved oil products as well as the gaseous products of liquefaction, such as significant amounts of carbon dioxide and water.

The liquefaction reaction of the LSW in tetralin with the dispersed iron/alumina-pillared clay catalyst (in situ sulfided) gave 30% conversion to heptane-solubles under the same conditions. The two-fold increase in conversion to oils for catalytic versus thermal reactions with the LSW substrate thus compares favorably with the increase of 6% (48 to 54%) found in the experiments with ion-exchanged coal described above.

The LSW intermediate was also subjected to the PETC iron dispersion treatment by stirring the low-density solid LSW with ferric nitrate solution and adding ammonium hydroxide to generate the surface-bound iron hydroxyoxide. The conversion of this material under conditions identical to those above with in situ sulfidation gave 15% heptane-solubles, the same as the thermal reaction. It is not known yet whether the iron sulfide that forms in the reaction with LSW is able to activate hydrogen, or whether some acidic component is required at this stage of liquefaction. This result may have very important implications for selecting conditions and coals for application of the PETC method to low-rank coals.

A variation of the PETC method was attempted to generate the dispersed iron catalyst on the LSW. Ethanol was used to obtain a colloidal dispersion of the LSW, which was then mixed with the ferric nitrate solution in ethanol and the ammonium hydroxide. After removal of the ethanol, the liquefaction was carried out in tetralin under conditions similar to those used above. When the dispersed iron obtained by this method was utilized, a 28% yield of heptane-soluble oils was obtained. It is now obvious that there are critical interactions between the iron and the coal surface that need to be

further elucidated and evaluated for designing a viable coal liquefaction method.

#### CONCLUSIONS

In coal liquefaction reactions that utilize dispersed iron catalysts, the catalytic activity was significantly improved by ion-exchange of cations present in the low-rank coals by aqueous acid-washing. Higher conversions to heptane-solubles were obtained with ion-exchanged Wyodak when dispersed iron catalyst was prepared by the PETC method. The ion-exchange pretreatment also improved the activity of the dispersed iron/alumina-pillared montmorillonite catalyst. A thermal pretreatment was also used to eliminate mineral matter, and the iron/alumina-pillared clay and one of the dispersed iron catalyst preparations were catalytically active.

#### 4.0 REFERENCES

1. Gollakota, S.V.; Vimalchand, P.; Davies, O.L.; Lee, J.M.; Corser, M.C.; Cantrell, Proceedings: Liquefaction Contractors' Review Meeting, U.S. Department of Energy Pittsburgh Energy Technology Center: Pittsburgh, 1991, pp 504-531.
2. Cugini, A.V.; Kratsman, D.; Hickey, R.F.; Lett, R.G., Abstracts: Liquefaction Contractors' Review Meeting, U.S. Department of Energy Pittsburgh Energy Technology Center: Pittsburgh, 1992, p 13.
3. Swanson, A.J.; Abstracts: Liquefaction Contractors' Review Meeting, U.S. Department of Energy Pittsburgh Energy Technology Center: Pittsburgh, 1992, p 8.
4. Joseph, J.T.; Forrai, T.R. Fuel 1992, 71, 75.
5. Olson, E.S.; Sharma, R.K. "Quarterly Technical Progress Report for the period July through September 1988", University of North Dakota Energy and Mineral Research Center: Grand Forks, ND, 1989.
6. Shams, K.; Miller, R.L.; Baldwin, R.M. Preprints: ACS Division of Fuel Chemistry, 1992, 37 (2), 1017-1024.
7. Cugini, A.V.; Utz, B.R.; Krastman, D.; Hickey, R.F.; Balsone, V. Preprints, ACS Div. of Fuel Chem. 1991, 36 (1), 91-102.
8. Olson, E.S.; Yaegelowich, M.L.; Sharma, R.K., Preprints: ACS Division of Fuel Chemistry, 1992, 37 (1), 262-267.
9. Ziolo, R.F.; Giannelis, E.P.; Weinstein, B.A.; O'Horo, M.P.; Ganguly, B.N.; Mehrotra, V.; Russell, M.W.; Huffman, D.R., Science 1992, 257, 219-222.

Table 2  
Catalytic Liquefaction with Iron/Alumina Pillared Clay

Reaction Temp. = 425°C, Reaction Time = 1 hr, H <sub>2</sub> = 1000 psi (cold) Coal/tetralin = 0.5, Catalysts = 10 wt%						
Coal (g)	Catalyst (wt. %)	Sulfur (g)	Conv. (g)	THF-I	Heptane-I	Heptane-S
Wyodak (AR) (7.0)	None	None	89	11	41	48
Wyodak (AR) (7.0)	APC-Fe <sub>3</sub> (10)	None	87	13	54	33
Wyodak (AR) (7.0)	APC-Fe <sub>3</sub> (10)	0.10	91	9	38	53
Wyodak (IEW) (5.34)	APC-Fe <sub>3</sub> (10)	0.10	95	5	41	54

AR = as received Wyodak  
IEW = 7.0 g AR coal was acid washed and dried

Table 3  
Catalytic Liquefaction of LSW Intermediate

Reaction Temp. = 425°C, Reaction Time = 1 hr, H <sub>2</sub> = 1000 psi (cold) Coal/tetralin = 0.5, Catalysts = 10 wt%					
Substrate (g)	Catalyst (wt. %)	Sulfur (g)	THF-I	Heptane-I	Heptane-S
LSW (1.0)	None	None	0	85	15
LSW (1.0)	APC-Fe <sub>3</sub> (10)	0.1	0	70	30
LSW (1.0)	PETC METHOD	0.10	0	73	28

## ACTIVITY OF SLURRY PHASE IRON-BASED CATALYSTS FOR HYDROGENATION AND HYDROCRACKING OF MODEL SYSTEMS

Ying Tang and Christine W. Curtis  
Chemical Engineering Department  
Auburn University, Alabama 36849-5127

### INTRODUCTION

Slurry phase catalysts have been shown to be very active for coal liquefaction. Pellegrino and Curtis (1989) compared the activity of three different types of molybdenum catalysts: an oil-soluble molybdenum naphthenate, a presulfided molybdenum on alumina, and a precipitated  $\text{MoS}_2$  catalyst. The catalyst generated *in situ* from molybdenum naphthenate was the most active in terms of hydrogenation and heteroatom removal as well as showing the highest coal conversion and product upgrading. Kim and Curtis (1990) evaluated catalyst precursors of molybdenum, nickel, and vanadium for their activity in coprocessing of coal with resid. The activity of the molybdenum and nickel precursors for coal conversion and oil production was high while that for the vanadium was low.

Comparisons of the catalytic activities of iron and molybdenum catalysts used in reactions of model coal molecules showed that  $\text{Fe}(\text{CO})_5$  or  $\text{Fe}(\text{CO})_5\text{-S}$  had high catalytic activity for hydrogenation of aromatic species (Suzuki et al., 1989). However,  $\text{Mo}(\text{CO})_6\text{-S}$  more strongly promoted hydrogenation of polyaromatic compounds as well as hydrogenation of some phenyl carbon bonds. The effect of dispersion methods had also been examined using iron catalysts in which an iron oxide ( $\text{FeOOH}$ ) precursor was dispersed onto the solid coal matrix (Cugini et al., 1991). Other iron systems, such as  $\text{Fe}_2\text{O}_3$  dispersed on carbon black, iron incorporated into coal by impregnating with  $\text{FeCl}_3$  and iron incorporated into lignite by cation exchange with a sulfated  $\text{Fe}_2\text{O}_3$ , have been used as finely dispersed catalysts for coal liquefaction and characterized by Mössbauer and XAFS spectroscopy (Huffman et al., 1991).

Finely divided iron (III) oxides and iron oxyhydroxides modified with either ( $\text{SO}_4^{2-}$ ) or molybdate ( $\text{MoO}_4^{2-}$ ) anions used in coal liquefaction have shown increased coal conversion and selectivities to n-pentane soluble products (Pradhan et al., 1991). A bimetallic catalyst,  $\text{Mo/Fe}_2\text{O}_3/\text{SO}_4^{2-}$  that consisted of 50 ppm Mo and 3500 ppm Fe, was active for coal conversion with a selectivity for oil. The effect of the pyrite to pyrrhotite ratio produced from ferric sulfide as a precursor on coal liquefaction has also been studied. A definite effect of intermediate stoichiometry of the ratio was observed on the selectivity to lighter products at higher liquefaction temperatures (Stansberry et al., 1991).

In this investigation, the effect of slurry phase iron catalysts on hydrogenation and hydrocracking reactions of model coal species was investigated. The areas investigated included (1) the effect of iron complex type on hydrogenation of pyrene and on hydrocracking of alkyl substituted naphthalenes; (2) the effect of different dispersion methods on catalytic activity of iron-based slurry catalyst precursors; and (3) the effect of combining iron with molybdenum slurry phase catalyst precursors on catalytic activity during the hydrogenation of pyrene.

## EXPERIMENTAL

The experimental reaction methods used for dispersing the catalyst precursors were (1) *in situ* where the catalyst precursor was added directly to the reaction system and reacted in the presence or absence of sulfur; (2) *ex situ* where the catalyst precursor reacted in the presence of the model compound was reclaimed and used in a second reaction and (3) two stages where the catalyst precursor was added to hexadecane, hydrogen, and sulfur and reacted for 30 min, then the model species was introduced into the reactor along with hydrogen and reacted for another 30 min.

**Pyrene Hydrogenation Reactions.** Iron slurry phase catalyst precursors were compared and utilized the *in situ* reaction method; molybdenum naphthenate was also used for comparison. The iron catalyst obtained *in situ* was generated by introducing the catalyst precursor at a level of 900 to 1100 ppm metal directly into the reaction system of 2 wt% pyrene in hexadecane. The reactants were charged into a 20 cm<sup>3</sup> stainless steel tubular microreactor and the reactions were conducted at 380 or 425°C for 30 or 60 min with a hydrogen pressure of 1250 psig at ambient temperature and an agitation rate of 550 rpm. Reactions were performed both with and without sulfur. When sulfur was present, it was introduced as elemental sulfur in a stoichiometric ratio of 3:1 sulfur to metal, presuming that either FeS<sub>2</sub> or MoS<sub>2</sub> was formed depending upon the precursor introduced.

The catalysts precursors used in the *in situ* experiments were iron (III) naphthenate, iron (III) acetylacetonate, iron (III) citrate hydrate, iron (III) 2-ethylhexanoate, iron (III) stearate, and molybdenum naphthenate for comparison. Iron (III) acetylacetonate (99% purity) was obtained from Eastman Kodak Company; iron (III) citrate hydrate (98% purity) was obtained from Aldrich Chemical Company; iron (III) 2-ethylhexanoate (8 to 11.5% Fe), iron (III) acetylacetonate (99% purity), and iron (III) stearate (9% Fe) were obtained from Strem; and the molybdenum naphthenate (6% Mo) was obtained from Shepherd Chemical. All of the catalyst precursors were used as received.

The *ex situ* catalyst was generated by collecting the catalyst solids produced during an *in situ* reaction and then drying the solids for 72 hours in a vacuum oven at 60°C. The dried solids were then introduced into the reactor containing pyrene in hexadecane solution at a level of 900-1100 ppm active metal. Hydrogen was introduced and the reaction was performed at the abovementioned conditions.

Two-stage pyrene hydrogenation reactions were performed by producing the catalyst in the first stage using a reaction system of catalyst precursor, excess sulfur, hexadecane, and a hydrogen pressure of 1250 psig at ambient temperature. After 30 min of reaction, the reactors were removed from the sandbaths, cooled, and then charged with pyrene and 1250 psig hydrogen introduced at ambient temperature. The pyrene hydrogenation reaction was then performed at 380°C for 30 min.

An analysis procedure UV-visible spectroscopy was developed for measuring the amount of organometallic complex that reacted under liquefaction conditions. The procedure developed used the metal complex dissolved in hexadecane as the reaction system. The concentration of the iron or molybdenum complex present after a given reaction time was determined by UV-visible spectroscopy. Each iron complex had to be dealt with differently in the experimental procedure because of their varying degrees of solubility in hexadecane. Iron naphthenate, iron 2-ethylhexanoate, and molybdenum naphthenate utilized hexadecane as a solvent for UV-visible spectroscopy. Iron citrate hydrate was dissolved in ethanol for analysis; iron acetylacetonate was

extracted with hot water for UV-visible analysis. For each metal complex, a calibration curve was developed using the same solvent for UV-visible analysis as was used after reaction.

The reactions using different amounts of iron and molybdenum complexes involved adding the different metal complexes *in situ* to the 2 wt% pyrene hydrogenation system. These experiments were performed at the same conditions as the previously described *in situ* reactions except that the iron and molybdenum complexes were added in weight ratios of 75:25, 50:50, and 25:75.

**Hydrocracking Reactions.** Two compounds were used as hydrocracking models: 1-methylnaphthalene and 2-hexylnaphthalene. 1-methylnaphthalene was obtained from Aldrich while 2-hexylnaphthalene was obtained from Dr. M. Farcasiu of PETC. The reaction system consisted of 2 wt% of the model compound dissolved in hexadecane. Three catalyst precursors were tested: iron naphthenate, iron stearate and molybdenum naphthenate; all of which were introduced at a level of 900 to 1100 ppm metal directly into the reaction system. Thermal baseline experiments were also performed. The reaction conditions were reaction temperatures of 380 or 425°C for 30 min with a hydrogen pressure at 1250 psig at ambient temperature and an agitation rate of 550 ppm.

**Analysis.** The reaction products obtained from the pyrene hydrogenation reactions were analyzed by gas chromatography using a Varian Model 3700 gas chromatograph equipped with FID detection and J&W DB5 30 m column. Quantitation was achieved by employing the internal standard method using p-xylene as the internal standard. The reaction products were identified comparing retention times with those of authentic compounds and by identifying unknowns by GC-mass spectrometry using VG70 EHF GC-mass spectrometer.

The product slates were determined for each reaction and the amount of hydrogenation of the aromatic determined. The percent hydrogenation is defined as the moles of hydrogen required to produce the product slate as a percentage of the moles of hydrogen required to produce the most hydrogenated liquid product. The most hydrogenated liquid product from naphthalene was considered to be decalin, from pyrene, perhydropyrene, from 1-methylnaphthalene, 1-methyldecalin and from 2-hexylnaphthalene, 2-hexyldecalin. Percent hydrocracking is defined as the mole percent of the products that have undergone hydrocracking.

## RESULTS AND DISCUSSION

**Pyrene Hydrogenation Reactions.** Of the five slurry phase catalysts tested for their activity for pyrene hydrogenation, Fe naphthenate (Fe Naph) was the most active while Fe stearate (Fe STR) showed equivalent activity at 425°C but lesser activity at 380°C (Table 1). Sulfur was required for any activity to be observed from either catalyst. The primary product obtained was dihydropyrene (DHP), the secondary products were hexahydropyrene (HHP), and small amounts of tetrahydropyrene (THP) were formed.

Of the other three slurry phase iron catalysts tested with sulfur, Fe AcAc reacted at 425°C was the only one which showed substantial pyrene hydrogenation of 9.3% and yielded the same products as Fe Naph. All of the other systems with sulfur, Fe citrate-hydrate (Fe CH) and Fe 2-ethylhexanoate (Fe 2-EH) showed limited activity for pyrene hydrogenation.

Reactions were also performed with Mo Naph with and without sulfur at 380 and 425°C for 30 min. The presence of sulfur in the reactor allowed the Mo released from Mo Naph to form finely divided MoS<sub>2</sub> which was an active catalyst for pyrene hydrogenation (Kim et al., 1989). At 380°C, without sulfur, the reaction with Mo Naph yielded 11.7% HYD with DHP

as the primary product and THP as the secondary product. At 380°C, with sulfur, the reaction with Mo Naph yielded 34.6% HYD of pyrene with HHP isomers being the primary products and a substantial amount of decahydroxyrene (DCHP) being formed.

At 425°C, the reaction of Mo Naph without sulfur showed less activity for pyrene hydrogenation than did the system with sulfur. Without sulfur the %HYD of pyrene was somewhat higher at 13.8% than at 380°C which yielded 11.7%. But the reaction at higher temperature, 425°C, with sulfur gave less activity than at 380°C with sulfur. At 425°C, thermodynamics are limiting the amount of pyrene conversion allowed and, hence, lower the amounts of partially saturated compounds produced in the reaction (Ting et al., 1992).

**Concentration of Iron Complexes at Liquefaction Conditions.** The iron complexes of Fe-CH, Fe Naph, Fe AcAc, and Fe 2-EH, each with an initial concentration of 1000 ppm Fe, were reacted at 380°C with an initial hydrogen charge of 1250 psig hydrogen introduced at ambient temperature. The concentration of each iron complex was determined by measuring the absorbance at two wavelengths and comparing the absorbance reading with a calibration curve for each complex obtained with the same solvent as was used with the reaction mixture. Each of the iron complexes disappeared very quickly at liquefaction conditions. After 5 min of reaction, all of the iron complexes were decomposed; in fact, all of them except Fe Naph were decomposed after 2 min of reaction. By contrast, Mo Naph remained in solution longer; after 10 min of reaction, more than half of the Mo Naph remained. However, Mo Naph had totally decomposed after 15 min of reaction.

**Comparison of Dispersion Methods for Activity of Fe Slurry Phase Catalysts.** Three methods of dispersion *in situ*, *ex situ*, and two stage batch processing were used to test the effect of dispersion on the catalytic activity of the generated catalysts (Table 2). Comparison of Fe Naph and Mo Naph activity for pyrene hydrogenation using the *in situ* method revealed that Mo Naph resulted in nearly three times as much hydrogenation as Fe Naph. HHP was the primary product for Mo Naph while DHP was the primary product for Fe Naph. The *ex situ* method, in which the catalyst produced in an *in situ* experiment was added to pyrene hydrogenation reaction system, resulted in less activity for both Fe Naph and Mo Naph. Fe Naph did not convert any pyrene while Mo Naph yielded about half the amount of hydrogenation observed in the *in situ* reaction.

Two-stage batch reactions were performed in which the catalyst precursor was introduced into hexadecane in the first stage and then reacted in the presence of sulfur and hydrogen for 30 min at 380°C. At that point, the reaction was quenched, gas released and pyrene and a new charge of hydrogen added. The system, including pyrene, was then reacted again for 30 min. The two-stage reaction with Fe Naph yielded about 6% conversion of pyrene to DHP so that its activity was much less than that of the *in situ* generated catalyst. By contrast, the two-stage reaction with Mo Naph yielded higher pyrene hydrogenation, 40% for the two-stage compared 34.6% for the *in situ* single-stage. Hence, the catalytic activity of Mo Naph appeared to increase with the two-stage treatment while Fe Naph did not.

**Effect of Combining Iron Complexes with Mo Naphthenate on the Reaction Products from Pyrene Hydrogenation.** Reactions were performed in which the catalyst precursors of the various iron complexes were combined with Mo Naph to determine if any synergism occurred in their catalytic activity for pyrene hydrogenation (Figure 1). Reactions were performed with 1000 ppm of the iron complex, 1000 ppm of Mo Naph, and with the combinations of 750 ppm iron complex with 250 ppm Mo Naph, 500 ppm with 500 ppm, and 250 with 750 ppm, respectively.

The combination of Fe Naph and Mo Naph at 75:25 and 50:50 Fe to Mo ratio yielded increased pyrene hydrogenation compared to either Mo Naph or Fe Naph alone. These results are presented in Figure 1 along with baseline experiments using Fe Naph and Mo Naph, individually. With Fe AcAc and Fe CH, each combined with Mo Naph, increased pyrene hydrogenation was observed at the combination of 25:75 Fe to Mo compared to the Mo Naph alone. By contrast, none of the combinations of Fe 2-EH with Mo Naph yielded increased conversions. In fact, the amount of pyrene hydrogenation increased with the amount of Mo Naph added; however, the amount of pyrene hydrogenation was less with Fe 2-EH than with Mo Naph alone at equivalent concentration levels. Therefore, for some combinations of Fe complexes and Mo Naph, synergism between the two catalyst precursors occurred resulting in increased pyrene hydrogenation, while another iron complex was detrimental to pyrene hydrogenation.

**Hydrocracking Reactions Using Fe Naphthenate and Fe Stearate.** Hydrocracking reactions using 1-methylnaphthalene (1-MN) and 2-hexylnaphthalene (2-HN) were performed using Fe Naph and Fe STR. The product distributions obtained with these reactions were compared to that obtained with naphthalene (NAP) (Table 3). The primary products obtained from 1-MN as shown in Table 3 were 5,6,7,8-tetrahydro-1-methylnaphthalene (5,6,7,8-1-MN) and 1,2,3,4-tetrahydro-1-methylnaphthalene (1,2,3,4-1-MN). For all catalysts the 5,6,7,8-1-MN isomer was the preferred product. At the higher reaction temperature, both iron complexes yielded NAP as a secondary product. If 1-methyldecalin is considered the most hydrogenated product, then the iron complexes both yielded between 6 and 7% hydrogenation of 1-MN but less than 3% hydrocracking. By contrast, Mo Naph yielded substantially more hydrogenation of ~26% but no hydrocracking. The baseline reaction using NAP only yielded tetralin (TET) as a product. No hydrocracking of the aromatic rings was obtained.

The reactions of 2-HN also given in Table 3 in the presence of Fe Naph, Fe STR and Mo Naph resulted in the production of two products: 2-hexyltetralin (2-HT) and 2-ethyltetralin (2-ET). For all three catalyst precursors, 2-HT was the primary product while 2-ET was the secondary product. Of all of the catalyst precursors, Mo Naph yielded the most hydrogenation and hydrocracking.

## SUMMARY

Slurry phase iron catalysts showed varying amounts of activity for pyrene hydrogenation reactions. Fe naphthenate and Fe stearate were the most active complexes although all of the Fe complexes broke down quickly at liquefaction conditions. By comparison, at the same reaction conditions, Mo naphthenate gave higher activity for pyrene hydrogenation. The activity of the slurry phase iron catalysts for pyrene hydrogenation depended upon the ligand type, reaction temperature and sulfur addition. The dispersion method also made a substantial difference in the activity of the catalyst. Fe naphthenate yielded the most activity using the *in situ* dispersion method and the least using the *ex situ* method. By contrast, Mo naphthenate showed the most activity with the two-stage process and the least with the *ex situ* method. Combination of some iron complexes with Mo naphthenate showed marked increases in activity for pyrene hydrogenation. In particular, the combination of Fe naphthenate with Mo naphthenate yielded increased yields of hydrogenated products from pyrene. Hydrocracking reactions revealed that the iron complexes promoted a small amount of hydrocracking with 1-methylnaphthalene and more with 2-hexylnaphthalene although Mo naphthenate promoted more hydrocracking of 2-hexylnaphthalene at equivalent reaction conditions.

## NOMENCLATURE

PYR = pyrene	Fe STR = iron stearate
DHP = dihydropyrene	Fe 2-EH = iron 2-ethylhexanoate
THP = tetrahydropyrene	Mo Naph = molybdenum naphthenate
HHP = hexahydropyrene	2-HN = 2-hexylnaphthalene
DCHP = decahydropyrene	2-HT = 2-hexyltetralin
1-MN = 1-methylnaphthalene	2-ET = 2-ethyltetralin
NAP = naphthalene	1,2,3,4-1-MN = 1,2,3,4-tetrahydro-1-methylnaphthalene
TET = tetralin	5,6,7,8-1-MN = 5,6,7,8-tetrahydro-1-methylnaphthalene
Fe Naph = iron naphthenate	%HYD = percent hydrogenation
Fe AcAc = iron acetylacetonate	
Fe CH = iron citrate hydrate	

## REFERENCES

- Cugini, A.V., Utz, B.R. Krustman, D., Hickey, R.I., Balsone, V. *ACS Fuel Chemistry Division Preprints*, 36(1), 91, 1991.
- Huffman, G.P., Ganguly, B., Taghili, M., Huggins, F.E. and Shah, N., *ACS Fuel Chemistry Division Preprints*, 36(2), 561, 1991.
- Kim, H., Curtis, C.W. *Energy and Fuels*, 4, 206-14, 1990.
- Kim, H., Curtis, C.W., *ACS Fuel Chemistry Division Preprints*, 35(4), 1990.
- Kim, H., Curtis, C.W., Cronauer, D.C., Sajkowski, *ACS Fuel Chemistry Division Preprints*, 34(4), 1431, 1989.
- Pellegrino, J.L., Curtis, C.W., *Energy and Fuels*, 3(2), 160, 1989.
- Pradhan, V.R., Herrick, D.E., Tierney, J.W., Wender, I. *Energy and Fuels*, 5(5), 712, 1991.
- Pradhan, V.R., Holder, G.D., Tierney, J.W. and Wender, I., "Modified Iron Oxide Catalysts in Coal Liquefaction," Fifth Annual Technical Meeting, Consortium for Fossil Fuel Liquefaction Science, Lexington, Kentucky, August, 1991.
- Stansberry, P., Zondlo, J.W., Yang, J., Stiller, A.H., Ragela, P., and Dadyburjor, D.B., "Ferric Sulfide as a Precursor for Coal Liquefaction," Fifth Annual Technical Meeting, Consortium for Fossil Fuel Liquefaction Science, Lexington, Kentucky, August, 1991.
- Suzuki, T., Yamada, H., Sears, P.L. and Watanabe, *Energy and Fuels*, 3, 707, 1989.
- Ting, P.S., Curtis, C.W., Cronauer, D.C. *Energy and Fuels*, 6, 511, 1992.

Table 1. Activity of Iron Complexes for Pyrene Hydrogenation

Product Distribution (mol %)	Fe Naphthenate		Fe Stearate		Fe Citrate-Hydrate		Fe Acetylacetonate		Fe 2-ethyl-Hexanoate	
	380°C	425°C	380°C	425°C	380°C	425°C	380°C	425°C	380°C	425°C
	3:1 S to Fe Ratio									
PYR	49.7±1.0	52.9±1.9	75.7±0.2	53.4±0.7	93.3±0.7	NP	95.6±0.7	61.6±0.6	100	90.5±0.7
DHP	32.1±0.5	29.1±0.5	18.2±0.2	26.7±0.6	6.7±0.7	NP	4.4±0.7	24.0±0.5	0	9.5±0.7
THP	2.9±0.1	3.2±0.3	0.0±0.0	3.2±0.4	0	NP	0	2.2±0.1	0	0
HHP	15.4±0.3	14.9±0.6	6.1±0.2	16.8±0.2	0	NP	0	12.3±0.2	0	0
% HYD	12.0±0.3	11.5±0.6	5.2±0.2	11.9±0.4	1.0±0.1	NP	0.6±0.1	9.3±0.1	0.0	1.4±0.1
	No Sulfur									
PYR	98.2±0.1	87.9±0.2	100.0	100.0	100.0±0	NP	98.8±0.8	93.1±0.5	100	94.2±0.2
DHP	1.8±0.1	12.1±0.2	0.0	0.0	0	NP	1.2±0.8	6.9±0.5	0	5.8±0.2
% HYD	0.3±0.0	1.7±0.0	0.0	0.0	0	NP	0.2±0.0	1.0±0.1	0.0	0.8±0.0

Reaction Conditions: 990-1100 ppm of Fe, 30 min, 1250 psig hydrogen pressure at ambient conditions, 2 wt % Pyrene in hexadecane.

Table 2. Comparison of Dispersion Methods of Iron and Molybdenum Precursors on Their Activity for Pyrene Hydrogenation

Product Distribution (mole %)	Fe Naphthenate			Mo Naphthenate		
	In Situ	Ex Situ	Two Stages	In Situ	Ex Situ	Two Stage
PYR	49.7±1.0	100.0±0.0	94.2±1.0	14.7±1.4	33.3	10.3±1.0
DHP	32.1±0.5	0.0	5.8±1.0	18.7±1.4	32.3	14.3±0.5
THP	2.9±0.1	0.0	0.0	7.5±0.6	9.1	6.2±0.3
HHP	15.4±0.3	0.0	0.0	43.5±0.9	25.5	45.8±0.8
DCHP	0.0	0.0	0.0	15.7±0.7	0.0	23.4±0.8
%HYD	12.0±0.3	0.0	0.8±0.1	34.7±1.7	18.1	40.2±0.6

**Table 3. Comparison of the Activity for the Hydrogenation and Hydrocracking of Naphthalene, 1-Methylnaphthalene, and 2-Hexylnaphthalene**

Product (mole %)				
	No Catalyst	Fe Stearate + S	Fe Naph + S	Mo Naph + S
<b>Naphthalene</b>				
NAP	100.0	85.5±0.4	83.9±0.5	
TET	0.0	14.5±0.4	16.1±0.5	
% HYD	0.0	5.8±0.1	6.4±0.1	
<b>1-Methylnaphthalene</b>				
1-MN	100±0.0	82.3±1.0	81.1±0.6	35.5±0.6
5,6,7,8-1-MN	0.0	11.9±1.0	10.8±0.5	39.2±0.8
1,2,3,4-1-MN	0.0	3.6±0.4	5.3±0.2	25.3±0.9
NAP	0.0	2.2±0.3	2.7±0.4	0.0
% HYD	0.0	6.3±0.4	6.6±0.3	25.8±0.4
<b>2-Hexylnaphthalene</b>				
2-HN	100.0±0.0	70.4±1.2	79.3±0.9	20.1±1.1
2-HT	0.0	16.5±1.2	11.1±0.9	43.5±1.0
2-ET	0.0	13.1±0.9	9.6±0.2	36.4±0.3
%HYD	0.0	14.8±0.7	10.4±0.8	40.0±1.0
%HYC	0.0	13.1±0.9	9.6±0.2	36.4±0.3

Reaction Conditions: 1250 psig H<sub>2</sub> introduced at ambient temperature; 30 minutes, 425°C, S to Fe ratio 3:1, S to Mo ratio 3:1.

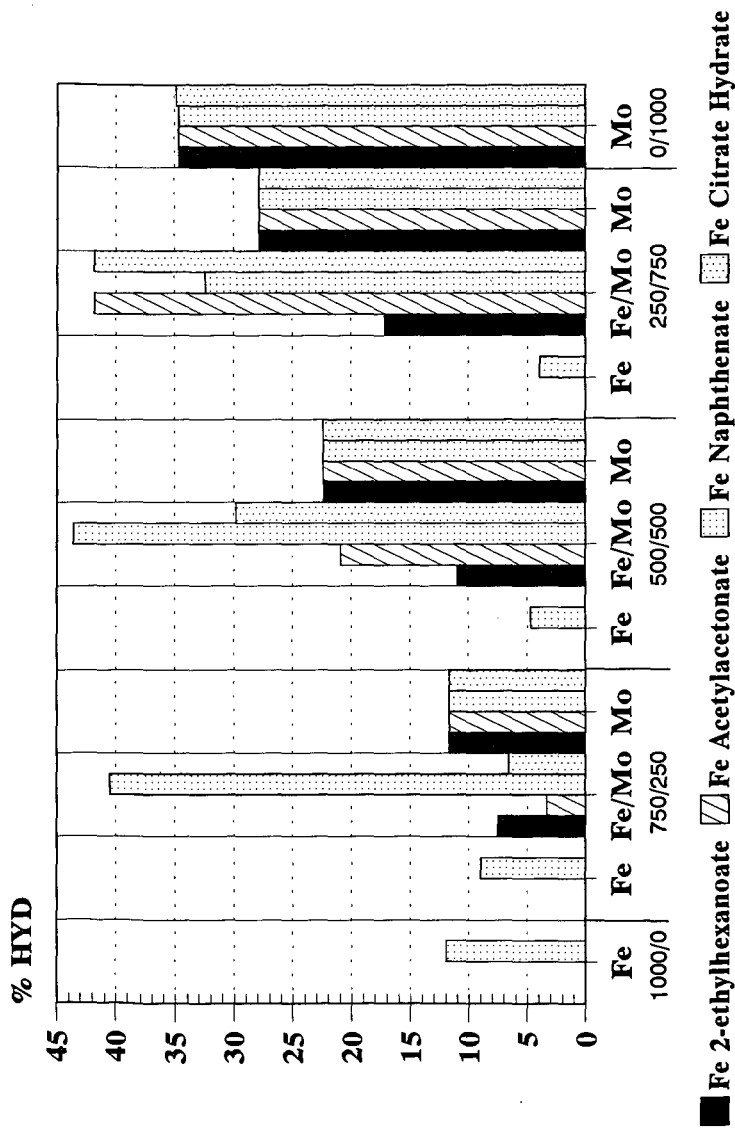


Figure 1. Synergism with Mo Naphthenate.

## CHARGE DISTRIBUTION ANALYSIS OF IRON OXIDE CATALYSTS\*

Friedemann Freund\* and Eun-Joo Whang

Department of Physics  
San Jose State University  
San Jose, CA 95192-0106

Keywords: Surface charge, Sign of charge carriers, Correlation with activity

### Abstract:

Catalytic reactions on solid contacts involve the exchange of charges across the solid/gas interfaces. Charge Distribution Analysis (CDA) is a new technique, capable of determining the generation of mobile charges in the bulk of materials and their appearance at the surface. By measuring the force acting on a sample in an electric field gradient, CDA derives unique information previously not available by any other technique. We have studied pressed pellets of two iron oxide catalysts supplied by the DOE Pittsburgh Energy Technology Center.  $\alpha$ - $\text{Fe}_2\text{O}_3$  (hematite), heated in  $\text{O}_2$ , behaves as a regular dielectric up to 450°C. The weakly negative surface charge indicates that electrons are the majority charge carriers. In  $\text{Fe}_3\text{O}_4$  (magnetite), heated in  $\text{N}_2$ , the surface is also weakly negative at ambient temperature, but evolves toward strongly positive values above 230°C. Upon cooling from 350°C this positive surface charge is firmly established, suggesting that defect electrons or holes have become the majority charge carriers. The trend toward positive surface charge continues up to 410°C when the composition of the magnetite sample starts to change. Between 275–410°C the magnetite is catalytically highly active toward dealkylation of 6-methyl-9-(1-methylethyl) dibenzo thiophene-4-ol. The fact that the catalytic activity toward dealkylation coincides with the appearance of a positive surface charge suggests that the active magnetite surface acts as an electron acceptor.

### INTRODUCTION

Whenever chemical reactions occur, they involve the transfer of electrical charges between reacting partners. When one of the partners is a solid and the reaction occurs catalytically at its surface, the onset of reactivity will be marked by the appearance of charge carriers in the bulk of the catalyst and their diffusive transport toward the active surface.

In principle, the appearance of charge carriers should be amenable to electrical conductivity measurements. However, conventional conductivity techniques require electrodes that are in direct contact with the sample surface. Obviously, this can cause many problems. If the electrode-sample contacts are good, the surfaces are no longer free and unperturbed. In the case of high surface area samples good physical contacts are impossible to establish. It is therefore fair to say that conventional electrical conductivity techniques appear not to be well suited to study catalytic reactivity – unless a method can be developed which allows contact-free measurement of the electrical conductivity.

\* Work supported by the ACS-Petroleum Research Fund under Grant #24335-AC5, the DOE Pittsburgh Energy Technology Center, and the NASA Ames Research Center.

\* Mailing address: NASA Ames Research Center, MS 239-4, Moffett Field, CA 94035-1000

## CHARGE DISTRIBUTION ANALYSIS - A POWERFUL NEW TECHNIQUE

*Charge Distribution Analysis* (CDA) is a non-contacting technique that allows conductivity measurements of insulating and semiconducting materials under minimum perturbation conditions <sup>1,2</sup>. CDA is based on the dielectric polarization at the limit of 0 Hertz. When a dielectric is placed in an external electric field of field strength  $E_{ext}$  it becomes polarized. Its polarization  $\mathbf{P}$  is:

$$\mathbf{P} = \frac{\epsilon_0(\epsilon-1)}{4\pi} \mathbf{E}_{ext} \quad (1)$$

where  $\epsilon_0$  is the permittivity of vacuum and  $\epsilon$  the dielectric constant.  $\mathbf{P}$  contains five contributions,  $\mathbf{P}_{el} + \mathbf{P}_{ion} + \mathbf{P}_{local} + \mathbf{P}_{space} + \mathbf{P}_{surface}$ , of which the first two refer to the ideal dielectric.  $\mathbf{P}_{el}$  reflects the electronic polarization of the electronic shells and  $\mathbf{P}_{ion}$  the ionic polarization due to the field-induced atom displacement. The remaining three contributions arise from defects and impurities.  $\mathbf{P}_{local}$  reflects local defects that change their intrinsic polarizability or dipolar defects that can rotate in the externally applied electric field.  $\mathbf{P}_{space}$  arises from the space charge polarization due to mobile charges that can diffuse inside the sample.  $\mathbf{P}_{surface}$  is uniquely related to the surface charge.

When a dielectric is placed in a field gradient along the z direction, a force  $\mathbf{F}_z^\pm$  acts on the sample towards higher field density. Using Maxwell's equations,  $\mathbf{F}_z^\pm$  is given to first approximation by:

$$\mathbf{F}_z^\pm = - \int \nabla (\mathbf{P} \cdot \mathbf{E}_{ext}) dV \quad (2)$$

where the volume integral includes the sample but not the sources of the field. In the case of an ideal dielectric (only  $\mathbf{P}_{el}$  and  $\mathbf{P}_{ion}$ )  $\mathbf{F}_z^\pm$  is invariant to the direction of the field gradient:  $\mathbf{F}_z^\pm = \mathbf{F}_z^+(\mathbf{E}_{ext}) = \mathbf{F}_z^-(\mathbf{E}_{ext})$ . In a real dielectric the contributions from  $\mathbf{P}_{local}$  and  $\mathbf{P}_{space}$  also remain invariant. However, the  $\mathbf{P}_{surface}$  term is variant to field gradient reversal. It causes an attraction to or repulsion from the region of higher field density, depending upon the sign of the surface charge. To separate ( $\mathbf{P}_{el} + \mathbf{P}_{ion} + \mathbf{P}_{local} + \mathbf{P}_{space}$ ) from  $\mathbf{P}_{surface}$  we form the linear combinations:

$$\mathbf{F}_\Sigma \equiv \frac{1}{2} (\mathbf{F}^- + \mathbf{F}^+) = - \frac{\epsilon_0(\epsilon-1)}{4\pi} \int \nabla \cdot \mathbf{E}_{ext}^2 dV \quad (3)$$

$$\mathbf{F}_\Delta \equiv \frac{1}{2} (\mathbf{F}^- - \mathbf{F}^+) = - \int \nabla (\mathbf{P}_{surface} \cdot \mathbf{E}_{ext}) dV. \quad (4)$$

To evaluate  $\mathbf{P}_{surface}$ , we introduce  $a_\pm U^2$  where  $a_\pm$  is a constant:

$$\mathbf{F}^\pm = \mathbf{F}_1^\pm + a_\pm U^2 \quad (5)$$

$a_\pm U^2$  describes the ideal dielectric and the  $\mathbf{F}_1^\pm$  are constants.  $\mathbf{F}_\Sigma$  and  $\mathbf{F}_\Delta$  are then given as:

$$\mathbf{F}_\Sigma = \frac{1}{2} (\mathbf{F}_1^- + \mathbf{F}_1^+) + \frac{1}{2} (a_- + a_+) U^2 \quad (6)$$

$$\mathbf{F}_\Delta = \frac{1}{2} (\mathbf{F}_1^- - \mathbf{F}_1^+) + \frac{1}{2} (a_- - a_+) U^2 \quad (7)$$

$\mathbf{F}_\Sigma$  characterizes the bulk polarization and is sensitive to the generation of mobile charges.  $\mathbf{F}_\Sigma$  is proportional to the square of the applied voltage.  $\mathbf{F}_\Delta$  characterizes the surface, its charge density and the internal electric field.  $\mathbf{F}_\Delta$  is linearly proportional to the applied voltage and its sign identifies the sign of the charge carriers, for instance electrons (negative) or holes (positive) that may be present in the catalyst sample.  $\mathbf{F}_\Sigma$  and  $\mathbf{F}_\Delta$  provide unique information about fundamental properties such as the on-set of chemical reactivity of a catalyst that is not available by any other known technique.

## EXPERIMENTAL

A PERKIN-ELMER TGS-2 thermobalance, equipped with a cup-shaped Pt-wound furnace (10 mm i.d. x 20 mm), was modified by the introduction of a circular bias electrode and a cylindrical ground electrode to create an asymmetrical capacitor of axial symmetry. The samples were suspended via a fused silica fiber, well insulated from ground, and placed into the region of the steepest electric field gradient, approximately 0.1–0.5 mm above the bias electrode. They were heated in 25°C increments, using a heating rate of 20°C/min. During the time at constant temperature the bias voltages were applied sequentially for 10–20 sec in increments of +20 V, 0 V and –20V. The forces were recorded as apparent weight changes in the sensitivity range 0.1–1 mg full scale.

The samples studied were coarse powders of  $\alpha$ -Fe<sub>2</sub>O<sub>3</sub> (hematite), labeled Catalyst #7, and Fe<sub>3</sub>O<sub>4</sub> (magnetite), which were both prepared by Dr. Malvina Farcasiu of the DOE Pittsburgh Energy Technology Center. The average grain size of the magnetite was 5  $\mu$ m and its specific surface area was of the order of 7 m<sup>2</sup>/g. Both powders were pressed dry into 6 mm diameter pellets, about 1.5 mm thick. The hematite was dried in N<sub>2</sub> at 150°C, heated in O<sub>2</sub> to 410°C, cooled to 380°C and reheated to 560°C. The magnetite was dried in N<sub>2</sub> to 150°C, then heated to 350°C ("2nd heating"). It was then cooled to 150°C and reheated to 500°C in N<sub>2</sub> with intermittent cooling from 400°C to 300°C and 450°C to 350°C ("3rd heating").

## RESULTS

$F_{\Sigma}$  of the hematite sample increased slightly and approximately linearly with temperature up to 500°C as shown in Fig. 1a. This suggests that up to 500°C, the sample behaved as a near-ideal insulator. Above 500°C, the  $F_{\Sigma}$  increased significantly, indicating that mobile charge carriers are being generated.  $F_{\Delta}$  was negative over the entire temperature range as shown in Fig. 1b, indicating that the surface charge of the hematite is dominated by electrons. A slight tendency towards positive  $F_{\Delta}$  values was noted after the intermittent cooling from 410°C to 380°C which, however, was overtaken by an even stronger trend towards negative  $F_{\Delta}$  values above 450°C. In conjunction with the pronounced increase in  $F_{\Sigma}$  above 500°C this response clearly suggests that the mobile charge carriers generated in the hematite above 450°C are electrons.

The magnetite exhibited a distinctly different behavior. As shown in Fig. 2a, the  $F_{\Sigma}$  values during the 2nd heating increased linearly with a lesser slope up to 230°C than above 230°C. This suggests the appearance of mobile charge carriers in the higher temperature range. During the 2nd heating,  $F_{\Delta}$  was initially very slightly negative and showed a trend towards more negative values up to 230°C as evidenced by Fig. 2b. Above 230°C, however, the trend reversed towards positive  $F_{\Delta}$  values.

After cooling to 150°C and subsequent reheating (3rd heating)  $F_{\Sigma}$  increased linearly from 230°C onward up to about 450°C with the same slope as during the 2nd heating as shown in Fig. 3a. During intermittent cooling and reheating cycles the  $F_{\Sigma}$  values were found to be successively higher, indicating that mobile charge had been generated during the heating cycles which did not disappear or recombine during cooling. Above 450°C,  $F_{\Sigma}$  increased more rapidly, but at the same time, the magnetite sample started to lose weight, probably due to changes in composition in the unbuffered N<sub>2</sub>

atmosphere. Experimentally this is seen in the fact that  $F_{\Sigma}$  is no longer proportional to the square of the applied bias voltage.

$F_{\Delta}$  remained positive during the 3rd heating as shown in Fig. 3b. Only at low bias voltage (20V) did  $F_{\Delta}$  still show the same trend towards negative values up to 230°C, followed by an evolution toward positive values. At the higher bias voltages the trend was towards positive values. During intermittent cooling up to about 410°C the positive  $F_{\Delta}$  values were further enhanced, indicating that the mobile charge carriers generated in the temperature interval 230–410°C have a positive sign. This in turn suggests that they are defect electrons or holes. The magnitude of  $F_{\Delta}$ , about 10% of  $F_{\Sigma}$ , indicates that the charge carrier density at the magnetite surface is rather high. However, quantitative data can be obtained only from single crystals, not from a pressed powder sample<sup>1</sup>. Above 410°C  $F_{\Delta}$  showed signs of degradation. Experimentally this is seen in the fact that  $F_{\Delta}$  was no longer linearly proportional to the applied bias voltage.

## DISCUSSION

The magnetite under study is active toward the dealkylation of 6-methyl-9-(1-methylethyl) dibenzo thiophene-4-ol in the presence of a hydrogen donor. In spite of its large average grain size (5  $\mu\text{m}$  diameter, 7  $\text{m}^2/\text{g}$  specific surface area), its catalytic activity is very high as illustrated in Fig. 4. The  $F_{\Delta}$  values shown (left ordinate) correspond to those measured during 2nd heating at 100V while the percentage dealkylation was achieved after 1 hour (right ordinate) using 25 mg catalyst and 25 mg 6-methyl-9-(1-methylethyl) dibenzo thiophene-4-ol. Trial runs performed by Dr. Farcasiu for 5 hrs at 150°C and 210°C did not produce an measurable dealkylation. Though we are still at an early stage of the investigation it appears that the catalytic activity of the magnetite may be directly related to the appearance of mobile charge carriers at its surface. The positive charge of the carriers identifies them as defect electrons or holes. Hence, the magnetite surface is expected to act as an electron acceptor.

Obviously, the holes are produced in the bulk of the magnetite crystals and diffuse to the surface where they become available for surface–gas reactions. To achieve the high turn–over number required for the observed degree of dealkylation, a large number of holes must flow from the bulk to the surface. By performing time–dependent CDA experiments it should also be possible in the future to measure the diffusive mobility of these active charges. Such measurements are of interest, if one tries to correlate the rate of a catalytic reaction with the density of charges at the solid surfaces.

On the basis of the data so far available, the CDA technique seems to be a promising tool to evaluate the activity of catalysts and to obtain valuable information about the nature of the charge carriers which participate in or are instrumental for catalytic reactions<sup>3</sup>.

## REFERENCES

- (1) Freund, M. M.; Freund, F.; Batllo, F. *Phys. Rev. Lett.* **1989**, *63*, 2096-2099.
- (2) Freund, F.; Batllo, F. *US Patent No. 4,884,031* **1989**,
- (3) Freund, F.; Maiti, G. C.; Batllo, F.; Baerns, M. *J. Chim. Phys.* **1990**, *87*, 1467-1477.

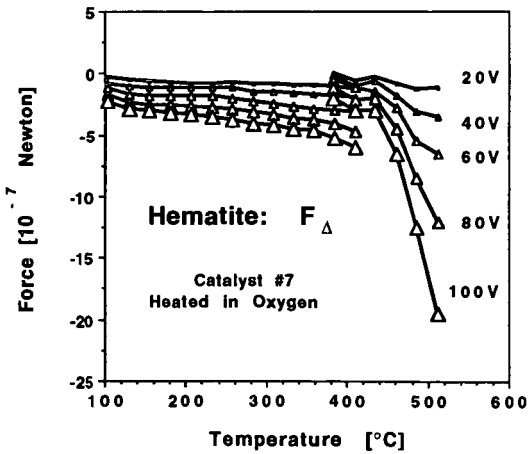
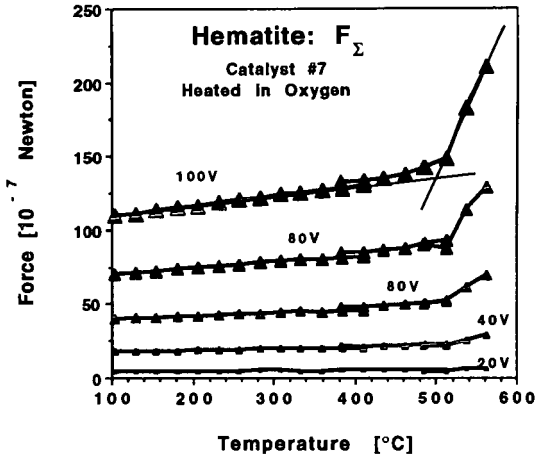


Fig. 1 a/b:  $F_{\Sigma}$  (top) and  $F_{\Delta}$  (bottom) of hematite (Catalyst #7) heated in  $O_2$ . The CDA response is typical for a near-ideal dielectric up to about 500°C. Throughout the temperature range studied, the dominant charge carriers are electrons.

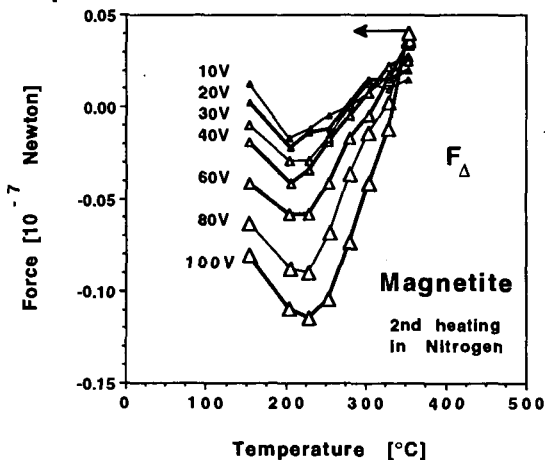
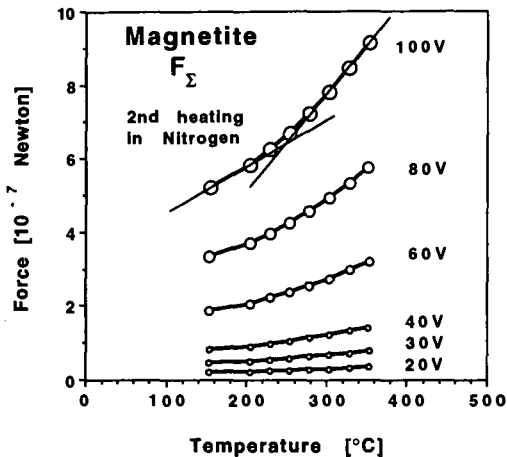
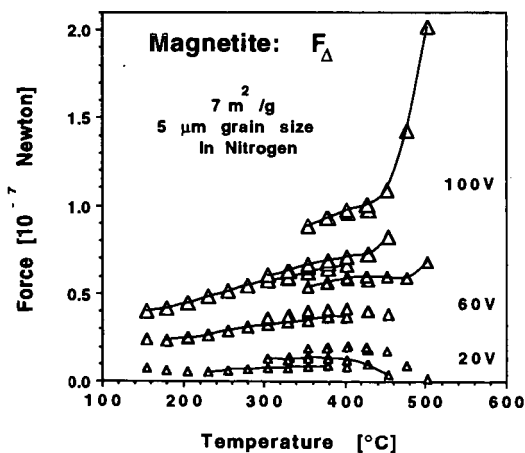
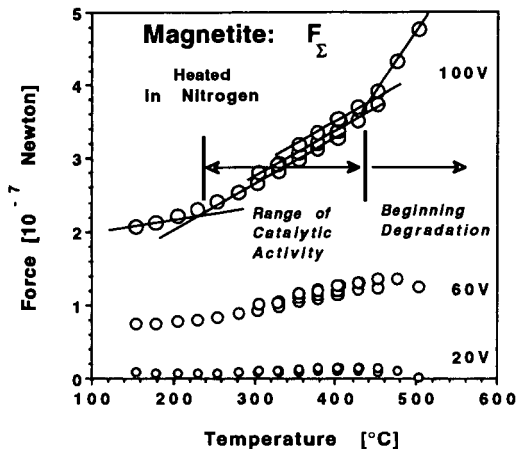


Fig. 2a/b:  $F_{\Sigma}$  (top) and  $F_{\Delta}$  (bottom) of magnetite heated in  $N_2$ . The CDA response suggests that, while electrons are the predominant charge carriers below  $230^{\circ}$ C, defect electrons or holes start to dominate at the higher temperatures.



**Fig. 3a/b:**  $F_{\Sigma}$  (top) and  $F_{\Delta}$  (bottom) of magnetite heated and intermittently cooled in  $\text{N}_2$ . The CDA response of magnetite suggests that defect electrons or holes are the predominant charge carriers up to  $450^{\circ}\text{C}$  at which point decomposition sets in.

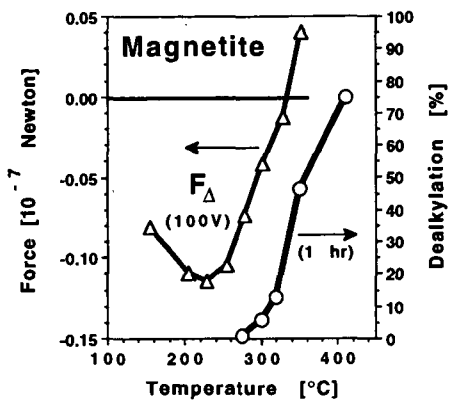


Fig. 4: Comparison between the surface charge of the magnetite sample in  $N_2$  as measured by CDA,  $F_{\Delta}$  (left scale), and the percentage of dealkylation of 6-methyl-9-(1-methylethyl) dibenzo thiophene-4-ol (right scale) after 1 hr. reaction time. At 150°C and 210°C no dealkylation occurred, even after 5 hrs. (Data courtesy of Dr. Malvina Farcasiu)

## FREE RADICAL INVESTIGATIONS OF DIRECT COAL LIQUEFACTION WITH Fe-BASED CATALYSTS USING ELECTRON SPIN RESONANCE SPECTROSCOPY

Manjula M. Ibrahim and Mohindar S. Seehra  
Physics Department, P.O. Box 6315  
West Virginia University, Morgantown, WV 26506-6315

Keywords: Coal hydrogenation; Free radicals; Fe-based catalysts

### ABSTRACT

Using a recently fabricated in-situ high pressure/high temperature electron spin resonance (ESR) apparatus, we report the variations of the ESR parameters of free radicals (density  $N$ , linewidth  $\Delta H$  and  $g$ -value) in the hydrogenation of Blind Canyon coal at 440°C and 415°C and as a function of  $H_2$  pressure up to 600 psi. More efficient hydrogenation is observed at 440°C as the decrease in  $N$  with  $H_2$  pressure is much higher at 440°C than at 415°C. A corresponding decrease in  $\Delta H$  with  $H_2$  pressure is also observed. Similar experiments but with loadings of  $Fe_2O_3/SO_4$  catalyst, elemental sulfur and hydrogen donor 9-10 dihydrophenanthrene are now being carried out.

### SUMMARY OF RESULTS/PROCEDURES

It is now generally accepted that direct coal liquefaction involves the interaction of thermally/catalytically generated free radicals in coals with the available hydrogen [1,2]. Some of these free radicals can be detected by in-situ electron spin resonance (ESR) spectroscopy. Recently we have fabricated a high pressure/high temperature in-situ ESR cavity system in order to investigate the free radical chemistry of direct coal liquefaction under more realistic conditions used in coal liquefaction experiments [3]. Experiments have been carried out from ambient to 500°C and for gaseous pressures up to 600 psi at X-band frequencies (~9 GHz). The density  $N$  of the free radicals and their  $g$ -values  $g$  and linewidth  $\Delta H$  are measured as a function of temperature and pressure. The experimental procedures for measuring these quantities have been described in a recent paper [4].

In Fig. 1, we show the variation of the free radical density  $N$  in Blind Canyon coal as a function of  $H_2$  pressure at two temperatures viz. 415°C and 440°C. The decrease in the free radical density with  $H_2$  pressure signifies hydrogenation since capture of  $H_2$  by free radicals quenches them and makes them undetectable by ESR. Comparing the results at 440°C with those at 415°C shows that hydrogenation is considerably more efficient at 440°C than at 415°C since considerably larger decrease in  $N$  with  $H_2$  pressure is observed at 440°C. The significance of these results is that these experiments are providing a direct evidence for the process of hydrogenation.

The variation of the  $g$ -value and the linewidth  $\Delta H$  of the free radicals with  $H_2$  pressure is shown in Fig. 2 for the experiments at 440°C. Whereas the  $g$ -value is essentially independent of  $H_2$  pressure, the linewidth decreases as the  $H_2$  pressure increases. The  $g$ -value, in favorable circumstances, can provide some information on the nature of the free radicals. However since there is no change in the observed  $g$ -value with  $H_2$  pressure (Fig. 2), no additional information on the chemical nature of free radicals is readily apparent from this experiment. The observed decrease in the linewidth with  $H_2$  pressure may be related to the decrease in the free radical density with  $H_2$  pressure observed in Fig. 1.

To simulate the conditions used in direct coal liquefaction, experiments are now underway in which the Blind Canyon coal is successively loaded with the catalyst (e.g.  $Fe_2O_3/SO_4$ ), elemental sulfur, and the hydrogen donor 9-10 dihydrophenanthrene (DHP). Free radical ESR

parameters are then monitored as a function of temperature in flowing H<sub>2</sub> gas and at fixed temperature as a function of H<sub>2</sub> pressure. In Fig. 3, we show one set of such results in flowing H<sub>2</sub> gas in which N vs T is plotted for the Blind Canyon coal, and for the coal loaded with Fe<sub>2</sub>O<sub>3</sub>/SO<sub>4</sub> and sulfur, and coal loaded with Fe<sub>2</sub>O<sub>3</sub>/SO<sub>4</sub>, sulfur and DHP. The loading by weight was in the ratio coal: Fe<sub>2</sub>O<sub>3</sub>/SO<sub>4</sub>:sulfur:DHP = 100:1.44:2.02:200. These loadings are chosen so as to give the ratios Fe/coal = 1/99 (~1%), Fe/S = 1/2, coal/DHP = 1/2. These preliminary results in Fig. 3 show that the catalyst and sulfur promote cracking since N is higher compared to the unloaded coal at all temperatures. With loading of DHP, magnitude of N is lowered as compared to the unloaded coal for temperatures below 260°C. Above this temperature, N values with DHP loading are essentially identical to the coal + catalyst + sulfur case as if the DHP is no longer present. To verify this, we carried out a thermogravimetric experiment on DHP in flowing H<sub>2</sub> gas. This experiment showed that by 290°C all DHP is evaporated, confirming the above argument. The lower values of N below 260°C in DHP are simply due to hydrogenation since it is well known that hydrogenation caps the free radicals, at least some of them. Experiments are now in progress under H<sub>2</sub> pressures up to 600 psi to simulate direct liquefaction conditions. Under H<sub>2</sub> pressures, evaporation of DHP at lower temperatures should be suppressed. Results of these experiments will be reported elsewhere in the near future.

#### ACKNOWLEDGMENTS

This research was supported in part by the U.S. Department of Energy through the Consortium for Fossil Fuel Liquefaction Science under DOE Contract No. DE-FC22-90PC90029.

#### REFERENCES

1. Neavel, R. C. *Fuel* 1976, 55, 237-242.
2. Petrakis, L. and Grandy, D. W. "Free Radicals in Coals and Synthetic Fuels" 1983 (Elsevier Science Publication Co. N.Y.).
3. Ibrahim, M. M. and Seehra, M. S., *ACS Div. Fuel Chem. Preprints*, 1992, 37, 1131-1140.
4. Seehra, M. S. and Ghosh, B. J. *Anal. Appl. Pyrolysis* 1988, 13, 209-220.

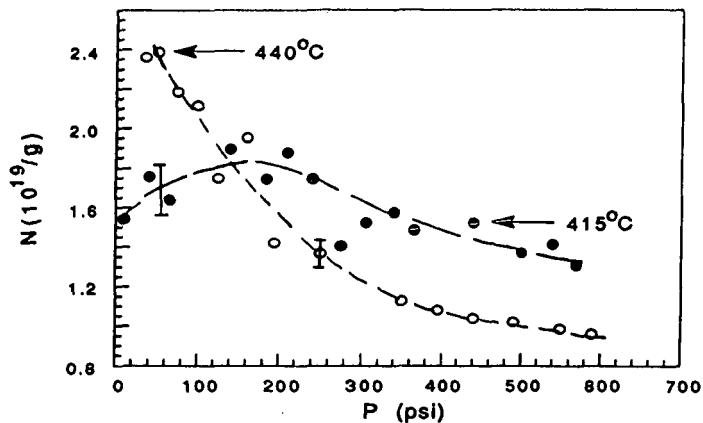


Fig. 1. Variation of N in Blind Canyon coal with  $H_2$  pressure at two temperatures.

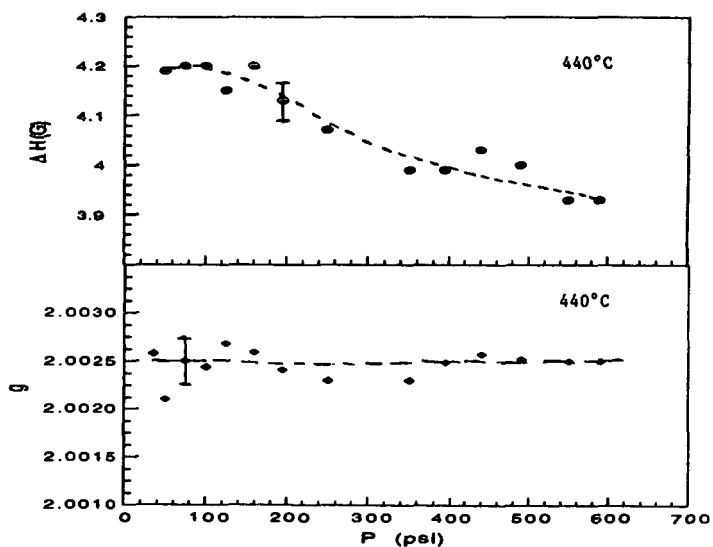


Fig. 2. Variations of the g-value and linewidth  $\Delta H$  with  $H_2$  pressure.

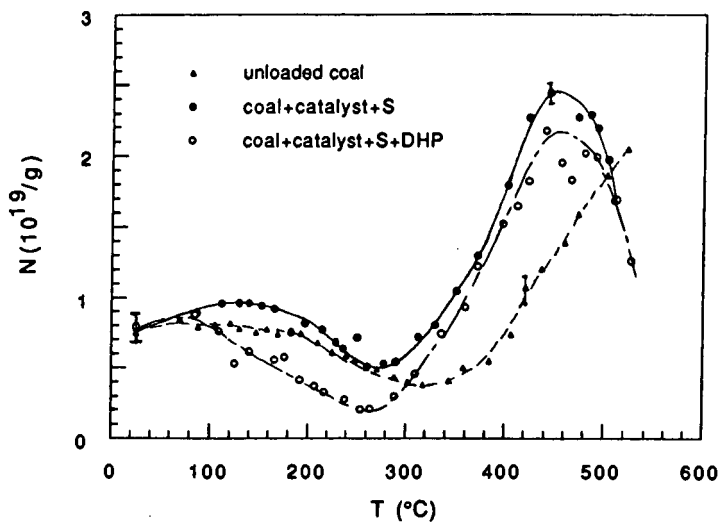


Fig. 3. Variation of free radical density  $N$  with temperature for unloaded and loaded coal. See text for details.